Nearfield broadband array design using a radially invariant modal expansion

Thushara D. Abhayapala and Rodney A. Kennedy
Telecommunications Engineering Group, Research School of Information Sciences and Engineering, Australian National University, Canberra ACT 0200, Australia

Robert C. Williamson
Department of Engineering, Faculty of Engineering and Information Technology, Australian National University, Canberra ACT 0200, Australia

(Received 22 December 1997; revised 5 February 1999; accepted 29 September 1999)

This paper introduces an efficient parameterization for the nearfield broadband beamforming problem with a single parameter to focus the beamformer to a desired operating radius and another set of parameters to control the actual broadband beampattern shape. The parameterization is based on an orthogonal basis set of elementary beampatterns by which an arbitrary beampattern can be constructed. A set of elementary beamformers are then designed for each elementary beampattern and the desired beamformer is constructed by summing the elementary beamformers with frequency and source-array distance dependent weights. An important consequence of our result is that the beamformer can be factored into three levels of filtering: (i) beampattern independent elementary beamformers; (ii) beampattern shape dependent filters; and (iii) radial focusing filters where a single parameter can be adjusted to focus the array to a desired radial distance from the array origin. As an illustration the method is applied to the problem of producing a practical array design that achieves a frequency invariant beampattern over the frequency range of 1:10 (which is suitable for speech acquisition using a microphone array), and with the array focused either to farfield or nearfield where at the lowest frequency the radial distance to the source is only three wavelengths.
 [S0001-4966(00)03901-1]

PACS numbers: 43.60.Gk, 43.38.Si, 43.30.Wi [JCB]

INTRODUCTION

Consider the problem of designing a microphone array for speech acquisition. Not only does the array require a narrow main beam, but it should operate uniformly over a large bandwidth and be able to cope with nearfield sources. While there has been a deal of progress in designing broadband arrays, having them operate well in the nearfield still requires rather *ad hoc* solutions. In this paper, we will present a systematic way of designing nearfield broadband sensor arrays. In particular, we will explicitly show how to parameterize the beamformer in order to focus the array to practically any operating radius from the array origin using a single parameter while maintaining a predetermined broadband angular beampattern using another set of parameters.

Most of the array processing literature assumes a farfield source having only plane waves impinging on the sensor array. However, in many practical situations, such as microphone arrays in car environments,[1] the source is well within the nearfield. The use of farfield assumptions to design the beamformer in these situations may severely degrade the beampattern. In many cases the approximate distance at which the farfield assumption begins to be valid is $r = 2L^2/\lambda$, where r is the distance from an arbitrary array origin, L is the largest array dimension, and λ is the operating wavelength.[2] However, we will show in Sec. I C that this common rule-of-thumb for farfield approximation is not a necessary condition.

There appears to be little work in the literature on nearfield beamforming. One method uses time delays to compensate for differing propagation delays due to spherical propagation.[3] However, this ignores the variation of the magnitude with distance and angle and assumes a point source. In another method,[4] there was consideration initially for nearfield theoretical development but this was ignored in the actual array design. The few other related works we are aware of dealing with design of nearfield arrays can be found in the references.[5–10]

A novel methodology to obtain precise nearfield array designs has been recently developed.[11] It is based on writing the solution to the wave equation in terms of spherical harmonics and allowing a nearfield beampattern specification to be transformed to the farfield, and the subsequent use of well understood farfield theory, to design the nearfield beamformer. These nearfield–farfield transformations have been used for many years in the radio antenna community for reconstructing farfield antenna patterns from nearfield measurements,[12] though these transformations are computationally involved. The theory of nearfield–farfield transformation was used to establish a computationally simple design procedure that numerically implements the nearfield–farfield transformation.[13] Farfield broadband beamforming has been considered[14–16] and reviewed in Ref. 14.

In this paper, a new method of beamforming is proposed in which an arbitrary desired beampattern in both frequency and angle may be produced either in nearfield or farfield. We have used the wave equation based representation of beampatterns[11] to identify the class of elementary beampat-

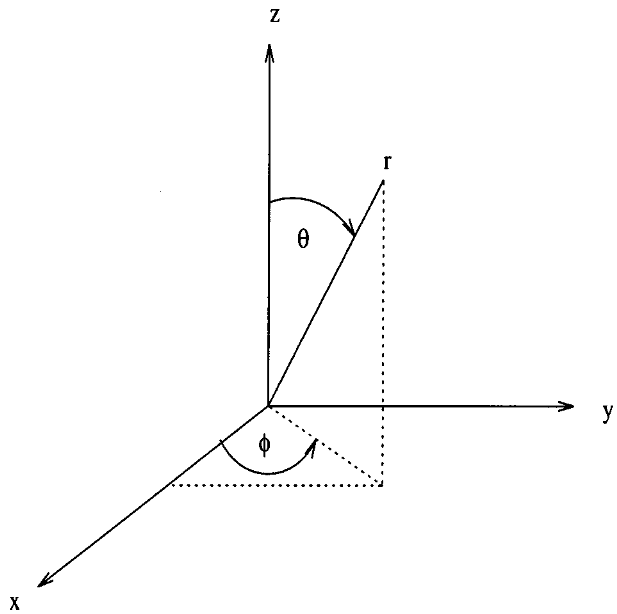

FIG. 1. Spherical coordinate system.

terns by which any arbitrary beampattern can be constructed. These elementary beampatterns form an orthogonal basis set. We use the concept of a theoretical continuous sensor to design elementary beamformers for each elementary beampattern. Then the desired beamformer is constructed by summing the elementary beamformers with frequency and radial distance dependent weights. The proposed beamformer structure has three major processing blocks: (i) a beampattern independent filtering block consisting of elementary beamformers; (ii) a beampattern shape dependent filtering block; and (iii) a radial focusing filter block, where a single parameter can be adjusted to focus the array to different radial distances from the array origin. Hence this design provides an efficient parametrization for adaptive beamformers, where only the beampattern shape dependent filters and a radial distance dependent parameter need to be adapted.

The paper is organized as follows: Section I introduces the notion of elementary shape invariant beampatterns as building blocks of beampatterns. The design of a general broadband theoretical continuous sensor as a sum of elementary continuous sensors is discussed in Sec. II. Section III shows how to approximate the theoretical continuous sensor by a practical discrete array of sensors. Guidelines for choosing the nonuniformly spaced sensor locations and the consequence of spatial sampling are addressed in Sec. IV. We conclude with an example broadband beamformer, which can be focused to either nearfield or farfield, in Sec. V.

I. THEORY OF ELEMENTARY SHAPE INVARIANT BEAMPATTERNS

A. Beampattern formulation

The nearfield–farfield transformation is obtained by solving the physical problem governed by the classical wave equation in the spherical coordinate system.[11] Let r denote radial distance, and ϕ and θ be the azimuth and elevation angles as shown in Fig. 1. Then a general valid beampattern is constructed by combination of all possible modes of the form[11]

$$r^{1/2}H^{(1)}_{n+1/2}(kr)P_n^{|m|}(\cos\theta)e^{jm\phi}, \tag{1}$$

where integers $n\geqslant 0$ and m (such that $|m|\leqslant n$) index the modes, $k=2\pi f c^{-1}$ is the wave number, f is the frequency of the wave, and c is the speed of wave propagation. The functions $P_n^m(\cdot)$ are associated Legendre functions and $H^{(1)}_{n+1/2}(\cdot)$ is the half-odd integer order Hankel function of the first kind which is defined by $H^{(1)}_{n+1/2}(\cdot)=J_{n+1/2}(\cdot)+jY_{n+1/2}(\cdot)$, where $J_{n+1/2}(\cdot)$ and $Y_{n+1/2}(\cdot)$ are the half-integer order Bessel functions of first and second kind, respectively. A property we will rely on is that there is no nonnegative integer n and no real number $r>0$ such that $H^{(1)}_{n+1/2}(r)=0$. This result follows from the fact that there are no common zeros for the functions $J_{n+1/2}(r)$ and $Y_{n+1/2}(r)$ (Ref. 17, p. 30).

The modes Eq. (1) are associated with waves propagating toward the origin (the half-odd integer order Hankel functions of the *second* kind give the waves propagating away from the origin). We assume that the propagation speed c is independent of frequency, implying k is a constant multiple of frequency f. Consequently, throughout this paper we will often refer to k as ''frequency.'' By combining modes for all possible n and m an arbitrary beampattern can be written as

$$b_r(\theta,\phi;k)=\sum_{n=0}^{\infty}\sum_{m=-n}^{n}\alpha_n^m(k)r^{1/2}H^{(1)}_{n+1/2}(kr)P_n^{|m|}(\cos\theta)e^{jm\phi}, \tag{2}$$

where $\{\alpha_n^m(k)\}$ is a set of frequency dependent coefficients. By introducing frequency dependence to the coefficients, we can use Eq. (2) to represent an arbitrary beampattern specification in both space (angle) and frequency. To complete the beampattern transformation model, it can be shown[11] that the $\alpha_n^m(k)$ coefficients can be obtained from the *analysis* equation:

$$\alpha_n^m(k)=\frac{(n+\frac{1}{2})}{2\pi r^{1/2}H^{(1)}_{n+1/2}(kr)}\frac{(n-m)!}{(n+m)!}\times\int_0^{2\pi}\int_0^{\pi}b_r(\theta,\phi;k)P_n^{|m|}(\cos\theta)e^{-jm\phi}\sin\theta\,d\theta\,d\phi. \tag{3}$$

Since we can invert the representation Eq. (2) via Eq. (3) we conclude that the $\alpha_n^m(k)$ uniquely represent an arbitrary beampattern. Equations (2) and (3) form an orthogonal transform pair. This implies the following linearity property which will be used later: if we have more than one beampattern at one fixed radius, then linearly adding them and transforming their sum to another radius is equivalent to the transformation of each beampattern separately to the second radius and then adding them together.

B. Elementary beampatterns

As we have seen in Eq. (2), any physically realizable beampattern can be constructed by combining modes of Eq.

(1). Inversely, an arbitrary beampattern can be decomposed into modes by Eq. (3). These modes in Eq. (1) are also valid beampatterns. Let us denote these beampatterns by

$$E_n^m(r,\theta,\phi;k) \triangleq R_n(r,k)\epsilon_n^m(\theta,\phi), \tag{4}$$

where

$$R_n(r,k) \triangleq r^{1/2} H_{n+1/2}^{(1)}(kr) \tag{5}$$

and

$$\epsilon_n^m(\theta,\phi) \triangleq P_n^{|m|}(\cos\theta) e^{jm\phi}. \tag{6}$$

The quantity $\epsilon_n^m(\theta,\phi)$ can be considered as an elementary beam shape and the quantity $R_n(r,k)$ is a complex function parameterized by distance r and frequency k. Therefore, the shape of the beampattern Eq. (4) is invariant with frequency as well as with distance. Hence we denote these beampatterns as *Elementary Shape Invariant Beampatterns* (ESIB). These are elementary because any physically realizable beampattern can be decomposed into a weighted sum of ESIBs:

$$b_r(\theta,\phi;k) = \sum_{n=0}^{\infty} \sum_{m=-n}^{n} \alpha_n^m(k) E_n^m(r,\theta,\phi;k), \tag{7}$$

where $\alpha_n^m(k)$ are the decomposition coefficients. From this point onward, we refer to Eq. (7) as the *modal representation* of beampatterns. Some examples of the lower order elementary beam shapes $\epsilon_n^m(\theta,\phi)$ for $m=0$ (which implies the shape is invariant with ϕ) are illustrated in Fig. 2 where the magnitude of $\epsilon_n^0(\theta,\phi)$ is plotted against θ. The shapes in Fig. 2 are the standard omni-directional, dipole, etc., patterns. It is evident that the number of *lobes* present is proportional to the mode n.

C. Radially invariant beampatterns

As a simple illustration of the modal representation Eq. (7), we now introduce a novel class of beampatterns related to ESIBs which are radially invariant with respect to their shape. A radially shape invariant beampattern $b_r(\theta,\phi;k)$ has the following property: For r_A, $r_B > 0$, $\theta \in [0,\pi]$ and $\phi \in [0,2\pi)$ there exists a complex constant $C \equiv C(r_A, r_B)$ such that

$$b_{r_A}(\theta,\phi;k) = C b_{r_B}(\theta,\phi;k). \tag{8}$$

One such class of beampatterns can be found excluding all but a single index n in Eq. (7) as

$$b_r(\theta,\phi;k)_{\text{invariant}} = R_n(r,k) \sum_{m=-n}^{n} \alpha_n^m(k) \epsilon_n^m(\theta,\phi), \tag{9}$$

where, in Eq. (8), the complex scaling factor $C = R_n(r_A,k)/R_n(r_B,k)$. Here, the shape of the beampattern is fixed with respect to radius r but its amplitude and phase are scaled with the distance from the array origin. However, this variation of phase and amplitude is same for all angles. The beampattern class Eq. (9) covers only a subset of all possible arbitrary beampatterns Eq. (7). An example of a beampattern of the form Eq. (9) is illustrated in Fig. 3. All radially invariant beam shapes of the form Eq. (9) need two-dimensional arrays [where $\alpha_n^m(k)=0$ for $m \neq 0$ in Eq. (9)] except trivial beam shapes such as omni-directional, dipole, etc.

The standard farfield design techniques can be applied to beampatterns such as Eq. (9) with the resulting beamformer automatically inheriting the radial invariance property if the farfield pattern is accurately realized. Note that the rule-of-thumb for farfield approximation[2] is not applicable for radial invariant beampatterns. For an arbitrary beampattern, the accuracy of this rule depends on the relative combination of ESIBs in Eq. (7).

A possible application of radially invariant beampatterns is in the microphone array design with a mixed nearfield/farfield problem,[10] where the array needs to focus to a nearfield source (the talker) but to attenuate farfield interference (reverberation). Keeping the same shape in both nearfield and farfield could be a useful solution to such a problem.

Radially invariant beampatterns are only one of the possible applications of ESIBs. In the remainder of this paper we will illustrate how ESIBs can be used to develop theory for more general broadband beamforming.

II. BROADBAND CONTINUOUS SENSOR DESIGN

A. Elementary continuous sensors

In previous sections we developed a new method for decomposing a given beampattern into elementary shape invariant beampatterns (ESIBs). We will now address the engineering problem of physically realizing these ESIBs using an array of sensors. We begin with the concept of *continuous sensor*, in order that an exact relationship between ESIBs and aperture illumination can be developed. The illumination function of the continuous sensor will then be approximated by a discrete sensor array to permit practical implementation.

In order to be able to completely describe results for different array configurations we introduce the notation $\rho(x,y,z;k)$ for the broadband aperture illumination or the response of the aperture at a point (x,y,z) and for a frequency k. The response of a continuous sensor to planar waves (i.e., those generated by a farfield point source) impinging from an angle (θ,ϕ) is then

$$b_\infty(u,v,w;k) = \int_{-\infty}^{\infty}\int_{-\infty}^{\infty}\int_{-\infty}^{\infty} \rho(x,y,z;k) e^{jk(ux+vy+wz)}\, dx\, dy\, dz, \tag{10}$$

where $(u,v,w) = (\sin\theta\cos\phi, \sin\theta\sin\phi, \cos\theta)$, $\theta \in [0,\pi]$ and $\phi \in [0,2\pi]$. Equation (10) is the standard three-dimensional Fourier transform relating the farfield beampattern to aperture illumination for a frequency k. The three-dimensional inverse Fourier transform corresponding to Eq. (10) is given by

$$\rho(x,y,z;k) = \left(\frac{k}{2\pi}\right)^3 \int\int\int b_\infty(u,v,w;k) \times e^{-jk(ux+vy+wz)}\, du\, dv\, dw, \tag{11}$$

where the three-dimensional integration is over the unit sphere.

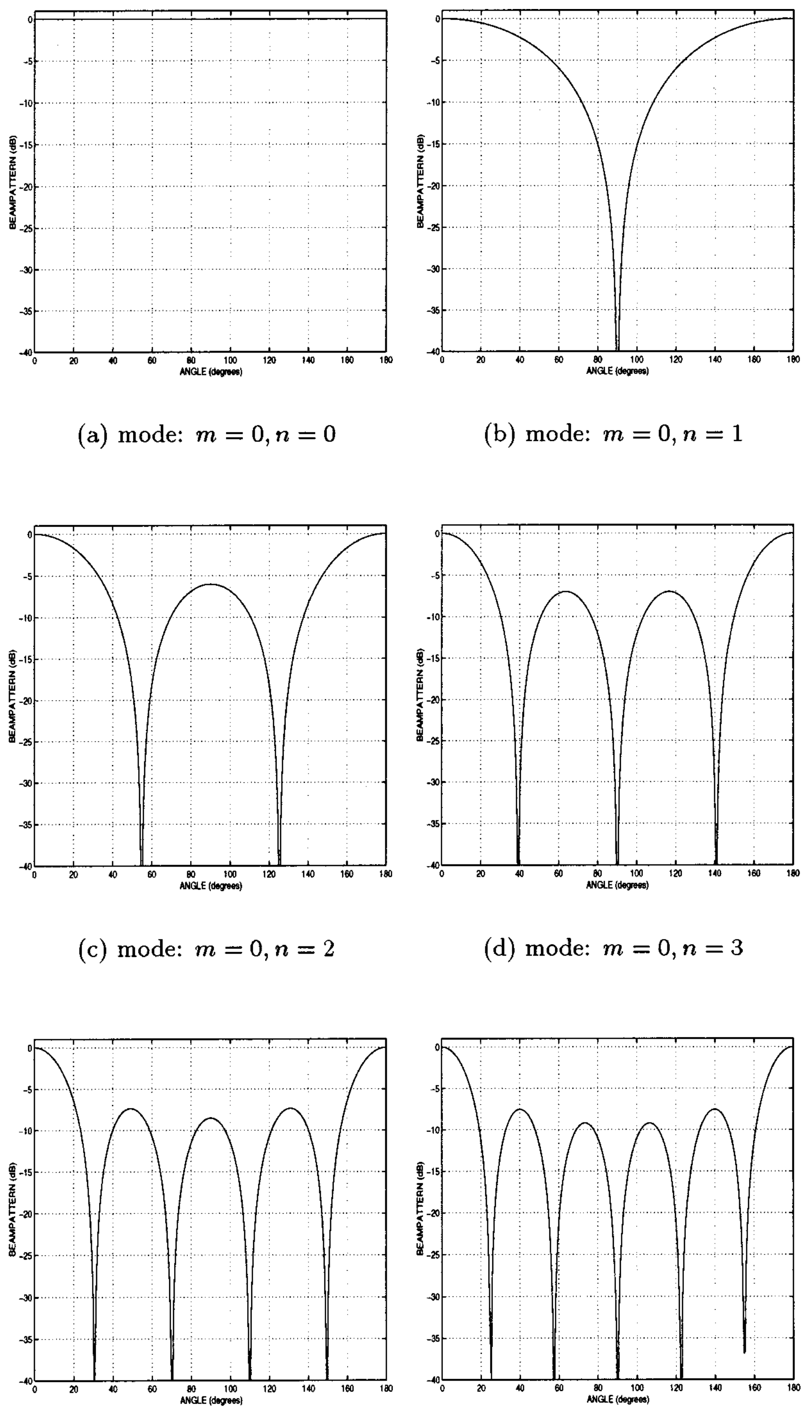

(a) mode: $m=0, n=0$ (b) mode: $m=0, n=1$

(c) mode: $m=0, n=2$ (d) mode: $m=0, n=3$

(e) mode: $m=0, n=4$ (f) mode: $m=0, n=5$

FIG. 2. Magnitude of few lower order elementary beam shapes $\epsilon_n^m(\theta,\phi)$ [given by Eq. (6)] for $m=0$ plotted against the angle θ. Note that these shapes are the standard omni directional, dipole, etc. patterns.

In order to establish an exact relationship between the ESIBs Eq. (4) and the aperture illumination function $\rho(x,y,z;k)$, we write an arbitrary farfield beampattern in the modal representation Eq. (7) as

$$b_\infty(u,v,w;k)=\sum_{n=0}^{\infty}\sum_{m=-n}^{n}\alpha_n^m(k)E_n^m(\infty,u,v,w;k), \quad (12)$$

where $\{\alpha_n^m(k):n\in\mathbb{Z}^+,\ \ m\in\mathbb{Z},\ \ |m|\leq n \ \text{ and } \ k\in\mathbb{R}^+\}$ are the decomposition coefficients and $E_n^m(\infty,u,v,w;k) \triangleq \lim_{r\to\infty} E_n^m(r,u,v,w;k)$ is the farfield beampattern given in Eq. (4) but expressed in the (u,v,w) coordinates. Substituting Eq. (12) into Eq. (11) and rearranging, we obtain the desired relationship as

$$\rho(x,y,z;k)=\sum_{n=0}^{\infty}\sum_{m=-n}^{n}\alpha_n^m(k)R_n(\infty,k)\varrho_n^m(x,y,z;k), \quad (13)$$

where

$$\varrho(x,y,z;k)\triangleq\left(\frac{k}{2\pi}\right)^3\int\int\int\epsilon_n^m(u,v,w) \times e^{-jk(ux+vy+wz)}\,du\,dv\,dw, \quad (14)$$

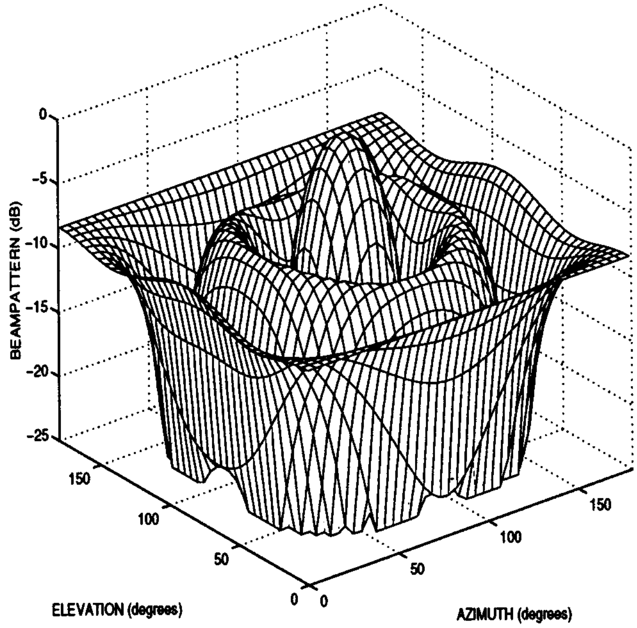

FIG. 3. An example of a shape invariant beampattern given by Eq. (9): $N=4$, $\alpha_4^4=0.05$, $\alpha_4^3=0$, $\alpha_4^0=0.35$, $\alpha_4^1=0$, $\alpha_4^0=7.0$, and $\alpha_4^{-m}=\alpha_4^m$.

and $R_n(\infty,k)\triangleq\lim_{r\to\infty}R_n(r,k)$. Using the results of Ref. 17 (p. 198) and Eq. (5) we have

$$R_n(\infty,k)=\lim_{r\to\infty} r^{1/2}H_{n+1/2}^{(1)}(kr)=(-j)^{n+1}\sqrt{\frac{2}{\pi k}}e^{j(k-k_0)}, \tag{15}$$

where k_0 is an arbitrary chosen nominal frequency. We can consider $\varrho_n^m(x,y,z;k)$ as the elementary aperture illumination functions. We can make following comments:

(1) An arbitrary farfield beampattern can be represented by Eq. (12). That means it can be decomposed in to ESIBs using Eq. (3) by calculating the coefficients $\alpha_n^m(k)$.
(2) Equation (14) could be used to find the elementary aperture illumination $\varrho_n^m(x,y,z;k)$ for each $\epsilon_n^m(\theta,\phi)$. Note that these elementary aperture functions are independent of the specific beampattern and they can be calculated beforehand in a practical situation.
(3) The coefficients $\alpha_n^m(k)$ have two interpretations: (i) they decompose the beampatterns Eq. (12) into a weighted sum of ESIBs, and (ii) they construct the aperture illumination Eq. (13) as a weighted sum of elementary aperture illumination functions.

B. Nearfield equivalence

In Sec. II A we introduced a technique to obtain a continuous aperture illumination function $\rho(x,y,z;k)$ for a broadband farfield beampattern using ESIBs. In this section, we generalize this result for broadband beampatterns at any radial distance from the array origin using the nearfield–farfield transformation technique.[11]

Theorem 1. *Let $b(\theta,\phi;k)$ be an arbitrary broadband beampattern specification. Then the aperture illumination, $\rho^{(r)}\times(x,y,z;k)$ of a continuous sensor which realizes this beampattern at a radius r from the sensor origin is given by*

$$\rho^{(r)}(x,y,z;k)=\sum_{n=0}^{\infty}\sum_{m=-n}^{n}\alpha_n^m(k)\frac{[R_n(\infty,k)]^2}{R_n(r,k)}\varrho_n^m(x,y,z;k), \tag{16}$$

where the elementary aperture illumination functions Eq. (14) $\varrho_n^m(x,y,z;k)$ and the complex functions $R_n(\cdot,k)$ [see Eq. (5)] are independent of the given beampattern and $\alpha_n^m(k)$ are the modal coefficients which give rise to the beampattern $b(\theta,\phi;k)$ in the farfield.

The proof is given in the Appendix. The theorem provides a method to achieve a desired beampattern response at any radius r from the array origin by a single parameter r adjustment of the continuous sensor $\rho^{(r)}(x,y,z;k)$.

C. One-dimensional sensor

The broadband array theory developed in the previous section is sufficiently general to capture quite arbitrary three-dimensional sensor geometries. In an attempt to bring the result into focus and provide a more concrete presentation of the ideas we examine a linear sensor aligned with the z axis. Specifically, we derive a closed form expression for the elementary aperture functions in the one-dimensional case. In this case, the beampattern is rotationally symmetric with respect to ϕ, and a farfield beampattern can be expressed as $b_\infty(\theta;k)=b_\infty(\theta,\phi;k)$.

By symmetry, the only nonzero components of the representation Eq. (12) are those for which $m=0$. Thus we obtain

$$b_\infty(\theta;k)=\sum_{n=0}^{\infty}\alpha_n(k)R_n(\infty,k)P_n^0(\cos\theta), \tag{17}$$

and

$$\rho^{(r)}(z,k)=\sum_{n=0}^{\infty}\alpha_n(k)\frac{[R_n(\infty,k)]^2}{R_n(r,k)}\varrho_n^0(z;k), \tag{18}$$

where $\alpha_n(k)\triangleq\alpha_n^0(k)$ and $\varrho_n^0(z;k)$ are the elementary aperture functions and $\rho^{(r)}(z,k)$ is the aperture illumination which will realize the desired response at a radius r from the array origin. By evaluating the integral in Eq. (14) for this case, we obtain a closed form expression for the elementary aperture functions for a linear sensor aligned with the z axis as:

$$\varrho_n^0(z;k)=\frac{k}{2\pi}\int_{-1}^{1}P_n(w)e^{-jkwz}\,dw \tag{19}$$

$$=\frac{k}{\sqrt{2\pi}}(-j)^n\frac{J_{n+1/2}(kz)}{\sqrt{kz}}, \tag{20}$$

where $P_n(\cdot)$ is the Legendre function of order n. Thus we have an exact expression for elementary aperture functions, although they are infinite in length. In the following section, we show how to discretize and truncate the continuous aperture functions derived.

III. BROADBAND DISCRETE ARRAY DESIGN

A. Background

We will now show how to exploit the above ideas for broadband array design. An array is a finite set of identical, discrete, omni-directional broadband sensors arranged in a regular geometry. We will only consider one-dimensional sensor arrays, although the results can be generalized to two and three dimensions. We consider a double sided array aligned to the z axis. There are few techniques discussed in the literature[18,19] for discretization of a continuous sensor; we closely follow the procedure given in Ref. 14.

B. Approximation

An array of sensors can only approximate the continuous aperture distribution described by Eq. (18). In our formulation this reduces to a numerical approximation of the following integral representation, which gives the output frequency response of the ideal continuous sensor for an arbitrary signal, having the frequency response $S(z,k)$, impinging on the array at position z:

$$Y(k)=\int_{-\infty}^{\infty}\rho^{(r)}(z,k)S(z,k)dz. \tag{21}$$

We use the well-known Trapezoidal integration method as used in Ref. 14 to approximate Eq. (21) by

$$\tilde{Y}(k)=\sum_{i=-L}^{L} g_i\rho^{(r)}(z_i,k)S(z_i,k), \tag{22}$$

where $\{z_i\}_{i=-L}^{L}$ is a set of $2L+1$ discrete sensor locations and g_i is a spatial weighting term which is used to account for the (possibly) nonuniformly spaced sensor locations. The role of g_i is better understood at the end of Sec. IV, where g_i is expressed in terms of sensor locations. The above approximation introduces two kind of errors: (i) the physical array is finite in extent and thus an infinite length integral has been replaced by a finite length summation; (ii) two spatially continuous functions $\rho^{(r)}(z,k)$ and $S(z,k)$ are replaced by their corresponding spatially discrete counterparts and hence there is a possibility of spatial aliasing and quantization errors.

C. Beamformer structure

We can consider $\rho^{(r)}(z_i,k)$ in Eq. (22) as the frequency response of a filter attached to the sensor at point z_i. By combining Eqs. (18) and (22) we write,

$$\tilde{Y}(k)=\sum_{i=-L}^{L} g_i S(z_i,k)\sum_{n=0}^{\infty}\alpha_n(k)G_n(r,k)F_n^0(z_i,k), \tag{23}$$

where

$$F_n^m(z_i,k)\triangleq\frac{\sqrt{2\pi}}{k}\varrho_n^m(z_i;k), \tag{24}$$

$$G_n(r,k)\triangleq\frac{k}{\sqrt{2\pi}}\frac{[R_n(\infty,k)]^2}{R_n(r,k)}. \tag{25}$$

The filters $F_n^0(z_i,k)$ depend on the elementary beam shapes and the position of the sensors. Using Eqs. (20) and (24), we get

$$F_n^0(z_i,k)=(-j)^n\frac{J_{n+1/2}(kz_i)}{\sqrt{kz_i}}, \tag{26}$$

where $J_{n+1/2}(\cdot)$ is the half-odd integer order Bessel function. We will call $F_n^m(z_i,k)$ the *elementary filters* (consistent with same terminology of ESIBs and elementary aperture functions). As in the case of ESIBs, these elementary filters are same for all beamformers, thus they may be useful in developing an effective parameterization for adaptation of beampatterns. Figure 4 illustrates the magnitude of the frequency response of the elementary filters of the first six modes versus the product of wave number k and the distance z to the associated sensor. We now demonstrate an important result regarding the elementary filters as a consequence of Eq. (26). Note that in Eq. (26), $F_n^0(z_i,k)$ is a symmetric function of spatial variable z_i and of the frequency variable k. Thus, these elementary filters have a *dilation property*:

Theorem 2. *All elementary filter responses $F_n^0(z_i,k)$ of the same mode n at different sensor locations z_i are identical up to a frequency dilation. That is*

$$F_n^0(z_i,k)=F_n^0\left(z_0,\frac{z_i}{z_0}k\right), \tag{27}$$

where z_0 is a reference sensor location.

The proof is given in the Appendix. With the output of the double-sided one-dimensional broadband array as defined in Eq. (23) and the dilation property of the elementary filters Eq. (41), we are led to a block diagram as shown in Fig. 5.

Regarding the beamformer structure we can make following comments:

(1) The proposed general beamformer has three levels of filtering associated with it. The first level consists of elementary beamformers, which are shown inside the dashed-line boxes in Fig. 5. Each of the elementary beamformers consists of elementary filters of the same mode which are connected to different sensors but are related by the dilation property. As a consequence, we have a set of unique beamformers for each and every mode n. In other words, the elementary beamformer of mode n produces the ESIB of the mode n. Further, the elementary beamformers are independent of the required beampattern specifications.

(2) The characteristic coefficients $\alpha_n(k)$ form the second level of filtering. Since the $\alpha_n(k)$ determine the shape of the beampattern, we call them *Beam Shape Filters*.

(3) The final set of filters $G_n(r,k)$ are independent of sensor locations but dependent on the operating radius r and the mode, and can be simplified using Eqs. (5), and (15), and (25),

$$G_n(r,k)=\frac{(-1)^{n+1}}{\pi^{3/2}}\sqrt{\frac{2}{r}}\frac{e^{j2(k-k_0)}}{H_{n+1/2}^{(1)}(kr)}, \tag{28}$$

where k_0 is an arbitrary chosen nominal frequency. By adjusting the parameter r in $G_n(r,k)$, the beamformer

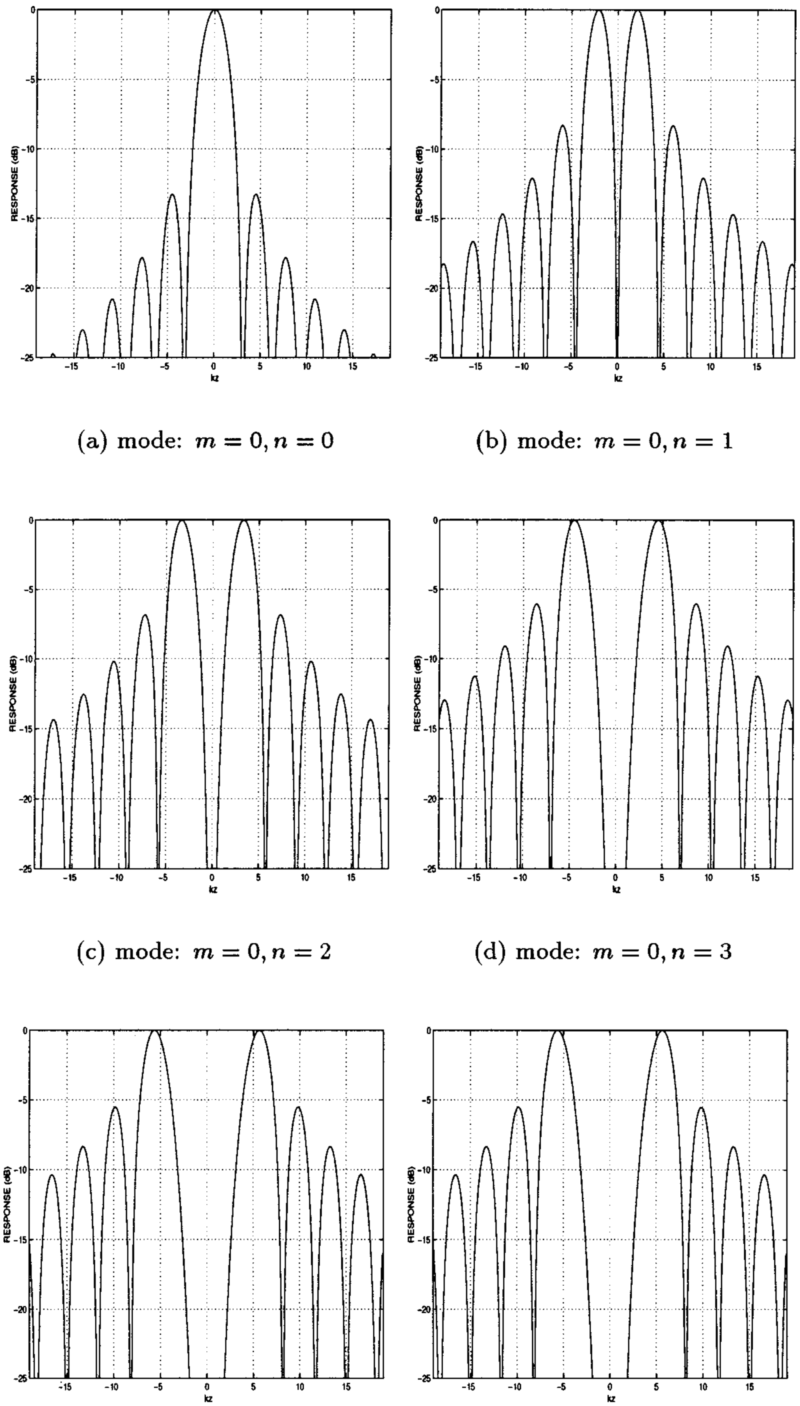

(a) mode: $m=0, n=0$ (b) mode: $m=0, n=1$

(c) mode: $m=0, n=2$ (d) mode: $m=0, n=3$

(e) mode: $m=0, n=4$ (f) mode: $m=0, n=5$

FIG. 4. Magnitude response of elementary filters $F_n^m(z,k)$ for $m=0$, plotted against the product of wave number k and the distance z to the associated sensor.

can be focused to a particular operating radius r either in nearfield or farfield. To highlight this important property we call the filters $G_n(r,k)$ *Radial Focusing Filters*.

(4) In Sec. I B we showed that an arbitrary beampattern can be decomposed into a weighted sum of ESIBs, where the weights are the characteristic coefficients $\alpha_n(k)$. Since each elementary beamformer produces an ESIB, an arbitrary beamformer can be implemented by adding them together with the decomposition coefficients $\alpha_n(k)$ of the required beampattern and the focusing filters $G_n(r,k)$. Because of these properties, our design is readily convertible to adaptive implementations, where only the beam shape filters and radial focusing filters need to be adapted.

(5) Finally, we will give some remarks about the general beamforming structure for two- and three-dimensional arrays. We can generalize the one-dimensional beamforming structure Eq. (23) for higher dimensions:

$$\tilde{Y}(k)=\sum_i g_i S(\mathbf{x}_i,k)\sum_{n=0}^{\infty} G_n(r,k)\sum_{m=-n}^{n}\alpha_n^m(k)F_n^m(\mathbf{x}_i,k), \tag{29}$$

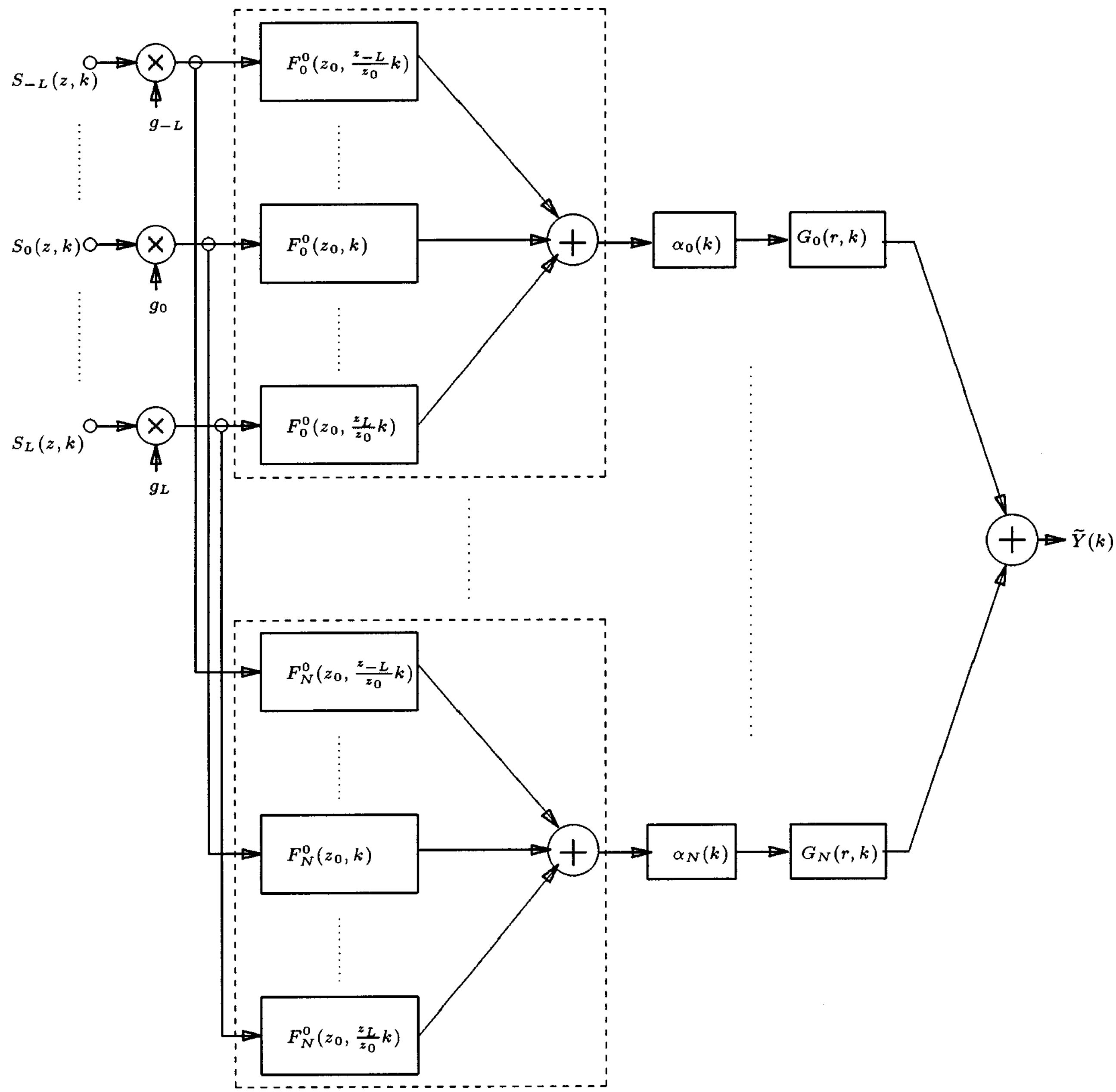

FIG. 5. Block diagram of a general one-dimensional broadband beamformer described by Eq. (23) where $F_n^0(z,k)$ is the elementary filters, $G_n(r,k)$ is the radial focusing filters, and $\alpha_n(k)$ are the beam shape filters.

where i is an integer and the sensors are placed at points $\{\mathbf{x}_i\}$ in the three-dimensional space. Let us assume that $\alpha_n^m(k)=0$ for $n>N$, where N is a positive integer. Then, there will be $N(N+2)$ elementary beamformers whose outputs are connected to the shape filters $\alpha_n^m(k)$. Compared with the one-dimensional beamformer (Fig. 5), there are additional summing points before the radial focusing filters $G_n(r,k)$ which add the outputs from the $(2n+1)$ shape filters $\alpha_n^m(k)$ of the same mode n but different m values.

D. Frequency invariant beamforming

We now consider the design of frequency invariant beamformers as a special case of the general beamforming theory developed above. This method generalizes the previous work.[14] The response of a frequency invariant beamformer is constant over an arbitrary design bandwidth. This type of beamformer is particularly useful for speech acquisition with microphone arrays.

An arbitrary beampattern over an arbitrary bandwidth can be expressed (in the farfield) by Eq. (17). It can be easily seen from Eq. (17) that if there is a sequence $\{\beta_n\}$ of mode dependent constants such that

$$\alpha_n(k)=\frac{\beta_n}{R_n(\infty,k)}, \tag{30}$$

for a range of frequencies $k\in[k_l,k_u]\subset(0,\infty)$, then the beampattern is frequency invariant over $k\in[k_l,k_u]$. This simplifies the general beamformer structure in Fig. 5, and in particular the product $G_n(r,k)\alpha_n(k)$ appearing in Eq. (23) can be simplified using Eqs. (25), (30), and (15):

$$G_n(r,k)\alpha_n(k)=\begin{cases}\beta_n\dfrac{k}{\sqrt{2\pi}} & \text{for farfield as } r\to\infty\\ \beta_n\dfrac{(-j)^{n+1}}{\pi}\sqrt{\dfrac{k}{r}}\,\dfrac{e^{j(k-k_0)}}{H^{(1)}_{n+1/2}(kr)} & \\ \quad\text{for nearfield at radius } r. & \end{cases}\tag{31}$$

Here, to determine β_n, we need only to calculate $\alpha_n(k)$ for some nominal frequency $k_0\in[k_l,k_u]$ and then use Eq. (30).

IV. CHOICE OF SENSOR LOCATIONS

As an engineering problem, it is desirable to minimize the number of sensors required while maintaining acceptable performance. The major factor determining the minimum number of sensors possible is *spatial aliasing*. It is well known from the array literature[20] that a sensor spacing of $\lambda/2=\pi/k$ is needed to avoid spatial aliasing for a narrow-band array operating at frequency k. For a broadband array, the upper limit of the design band frequency k_u must be used to avoid spatial aliasing in all frequencies, which suggests that a uniformly spaced array with π/k_u spacings is needed. However, such an array will give a smaller effective aperture for lower frequencies and larger aperture for a high frequencies which is undesirable. We will now show how to overcome this problem.

It has been shown,[13] by using the Parseval relation that the lower order modes (ESIBs) are the significant ones that give the broad beampattern features, whereas the higher order modes give the finer detail. We assert that sensible beampattern specifications should involve only the lower order modes. Hence, for most practical beampatterns, the characteristic coefficients $\alpha_n(k)$ are zero for larger n (typically $n>15$ or so). Let us assume $\alpha_n(k)=0$ for $n>N$, and thus we need to consider only ESIBs up to the mode N and the corresponding elementary filters.

We observe from Fig. 4 that the all elementary filters tend to have the characteristics of a bandpass filter except $n=0$ mode filter which has low-pass characteristics. Due to the dilation property of the elementary filters (see Theorem 2), the bandwidth and the cutoff frequencies of elementary filters are scaled with the location of the sensor to which they are connected. Therefore, as we move away from the origin, sensors become relatively inactive at higher frequencies. This means that the sensor spacings can be increased according to the highest frequency for which that sensor is effectively active. Consequently we can minimize the number of sensors as well as avoid the spatial aliasing.

For a given sensor location, the effective cutoff frequency of these filters increases as mode n increases. Let a_n be the product of the upper cutoff frequency $k_{c,n}$ of the mode n filter and the distance z to the associated sensor from the origin (i.e., $a_n=k_{c,n}z$), where $k_{c,n}$ is defined as the first zero crossing point above the pass band. (Note that these elementary filters are not ideal band pass filters and other definitions for cutoff frequencies such as half-power point can be used.) Table I lists the a_n of the first 16 elementary filters. Clearly the upper cutoff frequencies of elementary filters are related by $k_{c,1}<k_{c,2}<\cdots<k_{c,N}$. Therefore to make a sensor inactive for a given frequency k, it is sufficient to have $k_{c,N}<k$.

TABLE I. Upper cutoff frequencies of the first 16 elementary filters as a product of sensor location z and cutoff frequency $k_{c,n}$.

Mode (n)	$a_n=k_{c,n}z$
0	3.142
1	4.493
2	5.763
3	6.988
4	8.183
5	9.356
6	10.51
7	11.05
8	12.79
9	13.91
10	15.03
11	16.14
12	17.25
13	18.35
14	19.44
15	20.54

We can now give complete guidelines for choosing discrete sensor locations. Here we consider a double-sided array and begin with a sensor located at the array origin. Initially, to avoid spatial aliasing we need a sampling distance of $d_{k_u}=\lambda_u/2=\pi/k_u$. As long as the cutoff frequency k_i of the sensor located at z_i (which is equal to the cutoff frequency $k_{c,N}$ of the highest mode elementary filter attached to that sensor) is greater than the upper design frequency k_u, we need to maintain the above sampling distance. In this central portion of the array, the cutoff frequency of the ith sensor from either side of the origin is given by

$$k_i=\frac{a_N}{|i|\pi}k_u \quad \text{for } 0<|i|\le Q,$$

where Q is the number of uniformly spaced sensors in one side of the array. As we move further away from the origin, i.e., as i grows, k_i decreases and will become less than k_u. The number of uniformly spaced sensors Q required to satisfy this constraint is given by

$$Q=\left\lceil\frac{a_N}{\pi}\right\rceil,\tag{32}$$

where $\lceil\cdot\rceil$ is the ceiling function. At this point, we can increase the sampling distance, just to avoid spatial aliasing at k_Q. Since the cutoff frequency k_{Q+1} of the $(Q+1)$th sensor is less than that of Qth sensor, the sampling distance can be further reduced for the next location. This process can be continued until the cutoff frequency of the last sensor becomes less than the lower design frequency k_l. The result of this is that the location of the ith sensor relative to the origin is given by

$$z_i=\begin{cases}\dfrac{i\pi}{k_u} & \text{for } |i|\le Q\\ \dfrac{Q\pi}{k_u}\left(1+\dfrac{\pi}{\alpha_N}\right)^{|i|-Q} & \text{for } Q<|i|\le L,\end{cases}\tag{33}$$

where L is the total number of sensors in one side of the array. Using the fact that the cutoff frequency of the last sensor has to be less than or equal to the lower design frequency k_l, the number of minimum sensors per one side required to implement a broadband array over the design band is

$$L=Q+\left\lfloor\frac{\log\left(\frac{a_N k_u}{Q\pi k_l}\right)}{\log\left(1+\frac{\pi}{a_N}\right)}\right\rfloor, \tag{34}$$

where $\lfloor\cdot\rfloor$ is the floor function. Note that we need a total of $2L+1$ sensors altogether to have double-sided array.

In order to complete the guidelines for a practical realization of the beamformer given by Eq. (22), we now consider the spatial weighting term g_i introduced in Eq. (22). Recall that the Trapezoidal rule has been used to approximate the integral in Eq. (21) by the summation in Eq. (22), hence the spatial weighting term g_i is given by (possibly) nonuniform sensor locations Eq. (33) as

$$g_i=\begin{cases}\frac{1}{2}(z_{i+1}-z_{i-1}) & \text{if } |i|<L\\ \frac{1}{2}(z_L-z_{L-1}) & \text{if } |i|=L\end{cases}. \tag{35}$$

Note that any other integral approximation method can be used instead of Trapezoidal rule and the spatial weighting term g_i needs to be derived appropriately.

V. DESIGN EXAMPLE

We will now consider an example of broadband beamforming design using the techniques introduced above.

Suppose we wish to design a one-dimensional microphone array for operations in the air at sea level so $c=345\,\mathrm{ms}^{-1}$. Suppose the desired design frequency range is 300–3000 Hz, which is suitable for speech applications. Let us limit the maximum modes index N to be 15 as suggested in Sec. IV; thus we assume all beampatterns of our interest can be approximately decomposed to 16 ESIBs. Now we can determine the sensor locations and 16 elementary filters, which are independent of the desired response once the design band and the number of modes are decided. From Table I, the product of cutoff frequency $k_{c,n}$ and the sensor location z of the highest (15th) mode elementary filter is $a_N=20.54$. Next the sensors are placed according to Eq. (33) and it is found from Eq. (34) that the total number of sensors required is 41 and the length of the double-sided array is 4.9 m. The sensor locations are given in Table II and the frequency response of the elementary filters are given by Eq. (26).

Now we consider an example beampattern which is for a beamformer having a constant Chebyshev 25-dB beampattern (shown in Fig. 6) over the frequency range 300–3000 Hz. The example chosen is a frequency invariant beampattern, although we stress that our design method is not restricted to frequency invariant beamformers. The frequency responses of the combined filters $G_N(r,k)\alpha_n(k)$ are given by Eq. (31). For this case, the beampattern is characterized by the coefficients β_n and we have calculated them for $n=0,1,\ldots,15$ using Eqs. (38) and (3).

TABLE II. Locations z_i of the ith sensor of the example double-sided symmetric array in Sec. V (given in terms of the upper design wavelength λ_u).

i	z_i/λ_u
0	0.0
1	0.5
2	1.0
3	1.5
4	2.0
5	2.5
6	3.0
7	3.5
8	4.0
9	4.6
10	5.4
11	6.2
12	7.1
13	8.2
14	9.5
15	10.9
16	12.6
17	14.5
18	16.7
19	19.3
20	22.3

For the sake of efficient implementation, all the filters are collapsed into one filter per each sensor. This is possible, since the proposed beamformer structure (Fig. 5) consists of linear combinations of various filters.

The resulting beamformer is focused at the farfield by setting the parameter $r=100\lambda_l$ in the focusing filter $G_n(r,k)$. The response of the beamformer to a farfield source is given in Fig. 7(b), which is close to the desired response. The response of the same farfield focused beamformer to a nearfield source at a radius $3\lambda_l$ is given Fig. 7(a).

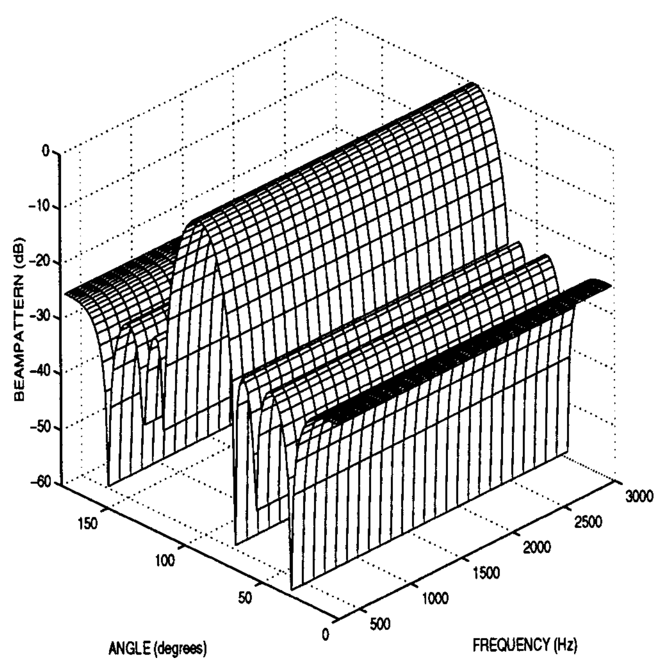

FIG. 6. Desired beamformer response used in the example in Sec. V: 25-dB Chebyshev beampattern over 300–3000 Hz.

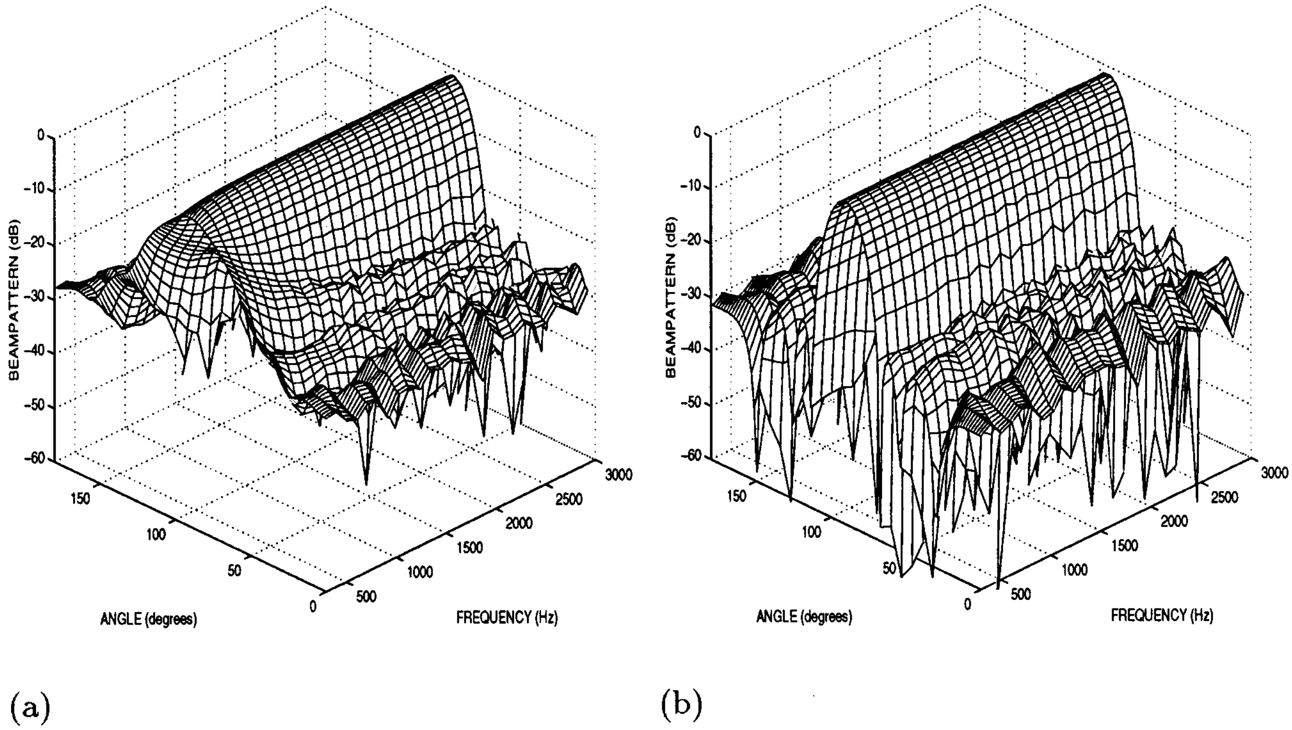

FIG. 7. Response of the farfield focused [by setting $r=100\lambda_l$ in the focusing filter $G_n(r,k)$] beamformer (see Fig. 5) with 25-dB Chebyshev beampattern to (a) a nearfield source at a radius $3\lambda_l$, (b) a farfield source at $100\lambda_l$. This figure demonstrates that the farfield design is inadequate for the desired nearfield performance.

It is evident from this figure that the farfield design is inadequate for the desired nearfield performance. Next we focus the same beamformer to the nearfield by simply adjusting the variable r in the focusing filter $G_n(r,k)$ to $3\lambda_l$. The resulting beamformer is simulated in the nearfield and we observe an improved response in Fig. 8(a). The focused array response is close to the desired response with neglible variation in the main beam and slight ripples in the side lobes. We conclude that the approximation involved in discretizing and truncating the continuous sensor was sufficiently accurate. For completeness, we find the response of nearfield focused beamformer to a farfield source and show this in Fig. 8(b).

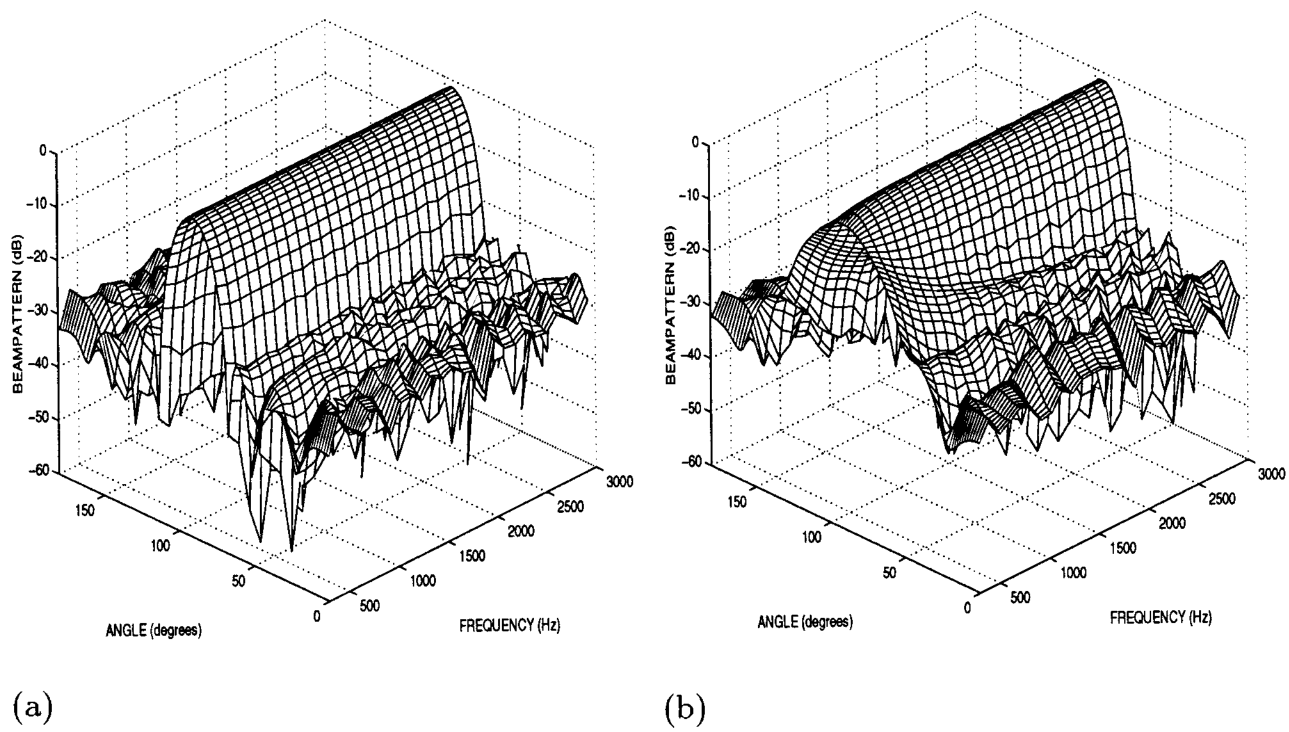

FIG. 8. Response of the nearfield focused [by setting $r=3\lambda_l$ in the focusing filter $G_n(r,k)$] beamformer (see Fig. 5) with 25-dB Chebyshev beampattern to (a) a nearfield source at a radius $3\lambda_l$, (b) a farfield source at $100\lambda_l$.

The similar appearance of Figs. 7(a) and 8(b) can be explained by our previous work[13] on radial reciprocity, which established the asymptotic equivalence of two transformation problems: (i) determining the nearfield performance of a farfield beampattern specification, and (ii) determining the equivalent farfield beampattern corresponding to a nearfield beampattern specification. We can view Figs. 8(b) and 7(a) as the result of problems (i) and (ii), respectively, with beampattern specification given in Fig. 6 for both cases.

VI. CONCLUSIONS

A new method of general broadband beamforming covering farfield and nearfield operations has been proposed in this paper. The efficient parameterization afforded by this technique enables the beamformer to be focused to a desired radial distance using a single parameter and the shape of the beampattern can be controlled by another set of parameters. These properties make it potentially useful for adaptive beamformer design.

APPENDIX

Proof of Theorem 1: Let $b_\infty(\theta,\phi;k)=b(\theta,\phi;k)$ be the beampattern specification in the farfield and let $a_{r_A}(\theta,\phi;k)=b(\theta,\phi;k)$ be a separate design with the same beampattern shape but at radius r_A (nearfield) from the sensor origin. Then we use Eqs. (2) and (4) to write,

$$b_\infty(\theta,\phi;k)=\sum_{n=0}^{\infty}\sum_{m=-n}^{n}\alpha_n^m(k)R_n(\infty,k)\epsilon_n^m(\theta,\phi), \quad \text{(A1)}$$

$$a_{r_A}(\theta,\phi;k)=\sum_{n=0}^{\infty}\sum_{m=-n}^{n}\beta_n^m(k)R_n(r_A,k)\epsilon_n^m(\theta,\phi). \quad \text{(A2)}$$

Note that the two sets of coefficients $\alpha_n^m(k)$ and $\beta_n^m(k)$ uniquely represent two different beampatterns, $a_r(\theta,\phi;k)$ and $b_r(\theta,\phi;k)$ in $(r,\theta,\phi;k)$ space. We will equate Eqs. (A1) and (A2) and observe that Eq. (A1) is the beampattern b_r evaluated at $r=\infty$ and Eq. (A2) is the beampattern a_r evaluated at $r=r_A$. Hence $\alpha_n^m(k)$ and $\beta_n^m(k)$ are related by $\alpha_n^m(k)R_n(\infty,k)=\beta_n^m(k)R_n(r_A,k)$ and thus

$$\beta_n^m(k)=\frac{R_n(\infty,k)}{R_n(r_A,k)}\alpha_n^m(k), \quad \text{(A3)}$$

since $R_n(r_A,k)=r_A^{1/2}H_{n+1/2}(kr_A)\neq 0$. Using the nearfield–farfield transformation, the farfield equivalent to a_{r_A} is given by

$$a_\infty(\theta,\phi;k)=\sum_{n=0}^{\infty}\sum_{m=-n}^{n}\beta_n^m(k)R_n(\infty,k)\epsilon_n^m(\theta,\phi). \quad \text{(A4)}$$

From Eq. (13) the aperture illumination function corresponding to this farfield pattern is

$$\rho(x,y,z;k)=\sum_{n=0}^{\infty}\sum_{m=-n}^{n}\beta_n^m(k)R_n(\infty,k)\varrho_n^m(x,y,z;k). \quad \text{(A5)}$$

Finally, by substituting Eq. (A3) into Eq. (A5) completes the proof.

Proof of Theorem 2: Let $F_n^0(z_0,k)$ and $F_n^0(z_i,k)$ be the frequency response of two elementary filters of the same mode n and associated with sensors at $z_0\neq 0$ and z_i, respectively. Then from Eq. (26),

$$\begin{aligned}F_n^0(z_i,k)&=(-j)^n\frac{J_{n+1/2}(kz_i)}{\sqrt{kz_i}}\\&=(-j)^n\frac{J_{n+1/2}\left(k\frac{z_i}{z_0}z_0\right)}{\sqrt{k\frac{z_i}{z_0}z_0}}\\&=F_n^0\left(z_0,\frac{z_i}{z_0}k\right),\end{aligned} \quad \text{(A6)}$$

which is a dilation in the frequency domain.

[1] Y. Grenier, ''A microphone array for car environments,'' Speech Commun. **12**, 25–39 (1993).
[2] R. J. Mailloux, *Phased Array Antenna Handbook* (Artech House, Boston, 1994).
[3] F. Khalil, J. P. Jullien, and A. Gilloire, ''Microphone array for sound pickup in teleconference systems,'' J. Aud. Eng. Soc. **42**, 691–700 (1994).
[4] J. L. Flanagan, D. J. Johnston, R. Zahn, and G. W. Elko, ''Computer-steered microphone arrays for sound transduction in large rooms,'' J. Acoust. Soc. Am. **78**, 1508–1518 (1985).
[5] F. Pirz, ''Design of wideband, constant beamwidth, array microphone for use in the near field,'' Bell Syst. Tech. J. **58**, 1839–1850 (1979).
[6] S. Nordebo, I. Claesson, and S. Nordholm, ''Weighted Chebyshev approximation for the design of broadband beamformers using quadratic programming,'' IEEE Signal Process. Lett. **1**, 103–105 (1994).
[7] M. F. Berger and H. F. Silverman, ''Microphone array optimization by stochastic region contraction,'' IEEE Trans. Signal Process. **39**, 2377–2386 (1991).
[8] J. G. Ryan and R. A. Goubran, ''Nearfield beamforming for microphone arrays,'' Proceedings of the IEEE International Conferences on Acoustic Speech Signal Processing, pp. 363–366 (Munich, 1997).
[9] J. G. Ryan and R. A. Goubran, ''Optimum nearfield response for microphone arrays,'' in *Workshop on Applications of Signal Processing to Audio and Acoustics*, Oct. 1997.
[10] D. B. Ward and G. W. Elko, ''Mixed nearfield/farfield beamforming: A new technique for speech acquisition in a reverberant environment,'' in *Workshop on Applications of Signal Processing to Audio and Acoustics*, Oct. 1997.
[11] R. A. Kennedy, T. D. Abhayapala, and D. B. Ward, ''Broadband nearfield beamforming using a radial beampattern transformation,'' IEEE Trans. Signal Process. **46**, 2147–2156 (1998).
[12] A. C. Ludwig, ''Calculation of scattered patterns from asymmetrical reflectors,'' Tech. Rep. 32–140, Jet Propulsion Laboratory, California Institute of Technology, Pasadena, California, Feb. 1970.
[13] R. A. Kennedy, D. B. Ward, and T. D. Abhayapala, ''Nearfield beamforming using radial reciprocity,'' IEEE Trans. Signal Process. **47**, 33–40 (1999).
[14] D. B. Ward, R. A. Kennedy, and R. C. Williamson, ''Theory and design of broadband sensor arrays with frequency invariant farfield beampatterns,'' J. Acoust. Soc. Am. **97**, 1023–1034 (1995).
[15] J. H. Doles III and F. D. Benedict, ''Broadband array design using the asymptotic theory of unequally spaced arrays,'' IEEE Trans. Antennas Propag. **36**, 27–33 (1988).
[16] M. M. Goodwin and G. W. Elko, ''Constant beamwidth beamforming,'' Proc. IEEE Int. Conf. Acoust. Speech Sig. Process. (ICASSP93), Vol. 1, pp. 169–172 (1993).
[17] N. W. McLachlan, *Bessel Functions for Engineers* (Oxford University Press, London, 1961).
[18] R. S. Elliott, ''On discretizing continuous aperture distributions,'' IEEE Trans. Antennas Propag. **AP-25**, 617–621 (1977).
[19] C. F. Winter, ''Using continuous aperture illumination discretely,'' IEEE Trans. Antennas Propag. **AP-25**, 695–700 (1977).
[20] J. L. Flanagan, ''Beamwidth and useable bandwidth of delay-steered microphone arrays,'' AT&T Tech. J. **64**, 983–995 (1985).